

Thermal Stress Analysis for Ceramics Stalk in the Low Pressure Die Casting Machine*

Nao-Aki NODA**, Hendra**, Yasushi TAKASE**
and Wenbin LI**

** Department of Mechanical Engineering, Kyushu Institute of Technology
Sensui-Cho 1-1 Tobata-Ku, Kitakyushu-Shi, Fukuoka, Japan
E-mail: noda@mech.kyutech.ac.jp

Abstract

Low pressure die casting (LPDC) is defined as a net shape casting technology in which the molten metal is injected at high speeds and pressure into a metallic die. The LPDC process is playing an increasingly important role in the foundry industry as a low-cost and high-efficiency precision forming technique. The LPDC process is that the permanent die and filling systems are placed over the furnace containing the molten alloy. The filling of the cavity is obtained by forcing the molten metal by means of a pressurized gas in order to rise into a ceramic tube, which connects the die to the furnace. The ceramics tube called stalk has high temperature resistance and high corrosion resistance. However, attention should be paid to the thermal stress when the stalk is dipped into the molten aluminum. It is important to develop the design of the stalk to reduce the risk of fracture because of low fracture toughness of ceramics. In this paper, therefore, the finite element method is applied to calculate the thermal stresses when the stalk is dipped into the crucible by varying the dipping speeds and dipping directions. It is found that the thermal stress can be reduced by dipping slowly if the stalk is dipped into the crucible vertically, while the thermal stress can be reduced by dipping fast if it is dipped horizontally.

Key words: Thermal Stress, Low Pressure Die Casting, Stalk, Molten Aluminum, FEM

1. Introduction

Low pressure die casting (LPDC) is especially suitable for producing axi-symmetric components such as light automotive wheels, cylinder head, piston and brake drum, etc. [1,2]. LPDC is defined as a net shape casting technology in which the molten metal is injected at a high speed and pressured into a metallic die. The LPDC process is playing an increasingly important role in the foundry industry as a low-cost and high-efficiency precision forming technique. Typically operating sequence for the LPDC is shown in Fig.1. The LPDC process is that the permanent die and filling systems are placed over the furnace containing the molten alloy. The filling of the cavity is obtained by forcing the molten metal by means of a pressurized gas in order to rise into a ceramic tube, which connects the die to the furnace.

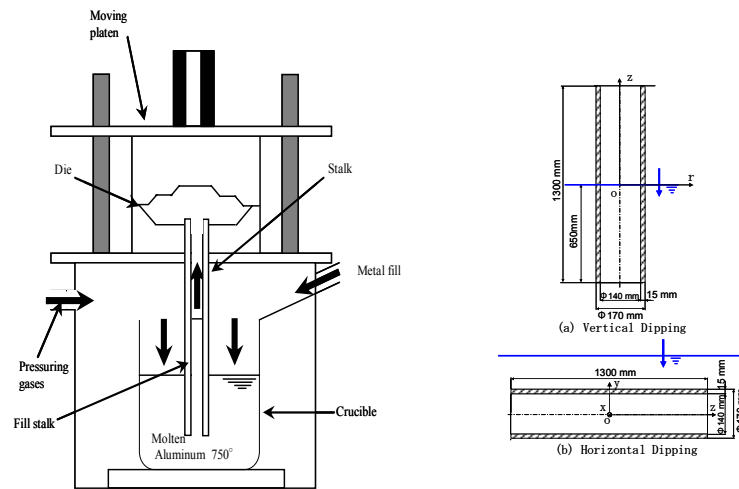


Fig.1 Schema of the low pressure die casting (LPDC) machine
(Note that LPDC is sometimes called “low pressure casting” in Japan)

The ceramic tube called stalk has high temperature resistance and high corrosion resistance. Previously, the tube was made of cast iron which resulted in spoiling the quality of product because of the partial melting of molten metal. Therefore, ceramics tube is introduced to improve the life time. However, there is still low reliability of ceramics

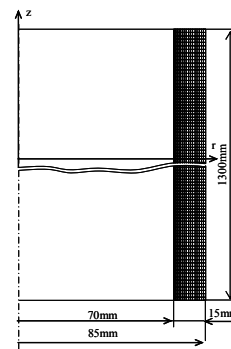


Fig. 2(a) Finite element mesh of vertical tube (No. of element=19500,
No. of nodes=20816)

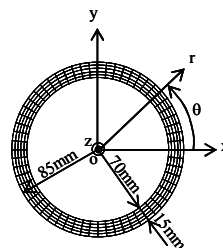
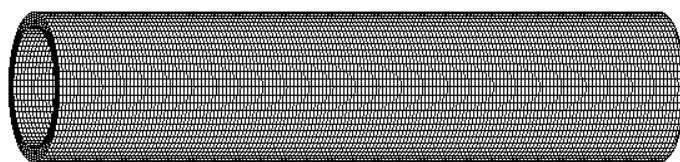


Fig. 2(b) Finite element mesh of horizontal tube (No. of element=45000,
No. of nodes=55986)

Table 1 The physical properties of molten aluminum at 750°C (1023K)

Physical property (dimension)	
Thermal conductivity λ , W/m K	112.2
Roll diameter D , m	0.17
Kinematics viscosity ν , mm ² /s	0.967
Isobaric specific heat C_p , kJ/kg K	1.1
Viscosity η , mPa s	2.2
Constants in Eq. (1) when $Re = 1 \times 10^3 - 2 \times 10^5$ (C_1)	0.26
Constants in Eq. (1) when $Re = 1 \times 10^3 - 2 \times 10^5$ (n)	0.6

Table 2 Mechanical properties of ceramics

Mechanical properties of ceramics (dimension)	Sialon
Thermal conductivity, W/m K	17
Specific heat, J/kg K	650
Coefficient of linear expansion, 1/K	3.0×10^{-6}
Young's modulus, GPa(kgf/mm ²)	294 (29979)
Specific weight	3.26
Poisson's ratio	0.27
4 Point bending strength, MPa (kgf/mm ²)	1050 (107)
Fracture toughness, MN/m ^{3/2}	7.5

mainly due to low fracture toughness.

As shown in Fig.1, the tube plays a critical function in the LPDC because it receives the molten metal from the crucible. However, attention should be paid to the thermal stress when the tube is dipped into the molten aluminum. It is important to reduce the risk of fracture because of low fracture toughness of ceramics. In this paper, therefore, the finite element method is applied to calculate the thermal stresses when the vertical tube is dipped into the crucible by varying dipping speeds and dipping directions. And, it will be compared with the previous research work done with horizontal tube analysis [3].

2. Analysis Method and Modeling

2.1 Analysis Model and Material Properties

In low pressure die casting machine in Fig.1, the tube is 170mm in diameter and 1300mm in length. Recently it is usually made of ceramic because of its high temperature resistance and high corrosion resistance. Temperature of the molten aluminum is assumed as 750°C, and the initial temperature of the tube is assumed as 20°C. Table 1 shows the physical properties of molten aluminum at 750°C (1023K) [4]. Table 2 shows the properties of ceramics called sialon [5,6] used for the tube. Axi-symmetric model will be used for vertical tube with total of 19500 elements and 20816 nodes as shown in Fig. 2(a). Three-dimensional model will be used for horizontal tube with total of 45000 elements and 55986 nodes as shown in Fig. 2(b). Here, 4-node quadrilateral elements will be employed for FEM analysis.

2.2 Evaluation for Surface Heat Transfer

To calculate the thermal stress, it is necessary to know the surface heat transfer coefficient α when the tube dips into the molten aluminum. Since three-dimensional thermo-fluid analysis to estimate α is very complicated, two-dimensional solutions will be considered. Zukauskas [7,8] proposed the following equation to estimate Nusselt number for a two-dimensional cylinder in the fluid with the velocity u .

$$Nu_m \equiv \frac{\alpha_m \cdot D}{\lambda} = C_1 \cdot Re^n \cdot Pr^{0.37} \cdot \left(\frac{Pr}{Pr_w} \right)^{0.25} \quad (1)$$

$$Re = \frac{u \cdot D}{\nu}, \quad Pr = \frac{C_p \cdot \eta}{\lambda} \quad (2)$$

Here, α_m is the average surface heat transfer coefficient, λ is thermal conductivity, D is the diameter of the cylinder, C_1 and n are constants determined by Reynolds number Re [9,10]. Also, Pr is Prandtl number, and subscript w denotes the property for temperature of cylinder wall. The velocity u can be calculated by the diameter of the tube divided by the time when the tube dips into the molten aluminum, which is usually, $u = 2 - 25\text{mm/s}$. The values of isobaric specific heat C_p , viscosity η , kinematics velocity ν are taken from reference [4], as shown in Table 1. Substituting these into Eqs. (1) and (2), Nu_m is given for the determination of α_m . Namely,

$$\alpha_m = 1.523 \times 10^3 \text{ W/m}^2 \cdot \text{K} \quad (\text{when } u = 2\text{mm/s}). \quad (3)$$

$$\alpha_m = 11.27 \times 10^3 \text{ W/m}^2 \cdot \text{K} \quad (\text{when } u = 25\text{mm/s}). \quad (4)$$

When a ceramic roll with a diameter of 250mm is dipping into molten zinc, we have used the following value in the previous paper [3].

$$\alpha_m = 4.6 \times 10^3 \text{ W/m}^2 \cdot \text{K} \quad (\text{when } u = 25\text{mm/s}) \quad (5)$$

Figure 3 shows the distributions of surface heat transfer coefficient as a function of x/a . The results for $a = 125\text{mm}$ in molten zinc were obtained by the application of the finite volume method for two-dimensional cylinder model in the molten metal with the velocity $u = 25\text{mm/s}$. The results of Fig. 3 will be used for vertical and horizontal tubes in Fig. 1 (a) and (b). Since the value of Eq. (4) is 2.45 times larger than the value of Eq. (5), the distribution for the tube $a = 85\text{mm}$ in molten aluminum is estimated from the results for $a = 125\text{mm}$ in molten zinc by multiplying by 2.45. In Fig.3, the average value for $a = 85\text{mm}$ is $\alpha_m = 10.9 \times 10^3 \text{ W/m}^2 \cdot \text{K}$ and the average value for $a = 125\text{mm}$ is $\alpha_m = 4.4 \times 10^3 \text{ W/m}^2 \cdot \text{K}$. They are in good agreement with Eqs. (4) and (5).

3. Thermal Stress for Vertical Tube

The vertical tube model with the length of 1300mm as shown in Fig.1(a) is considered when half of the tube is dipping into molten aluminum at the speeds of $u = 2\text{mm/s}$ and $u = 25\text{mm/s}$.

3.1 Results for Dipping Slowly

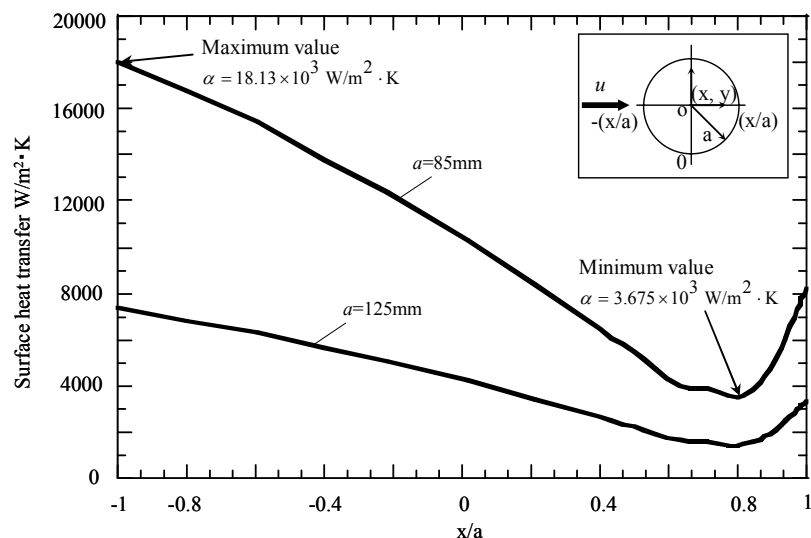
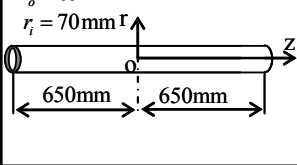
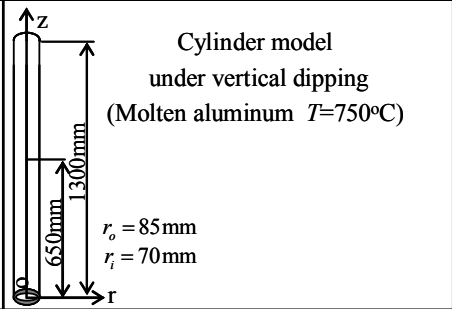
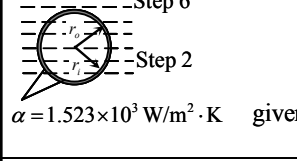
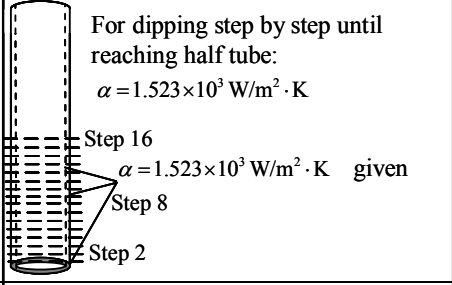

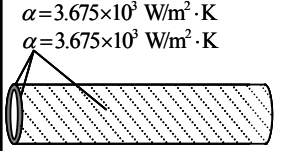
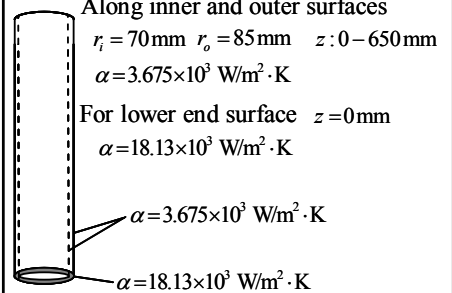
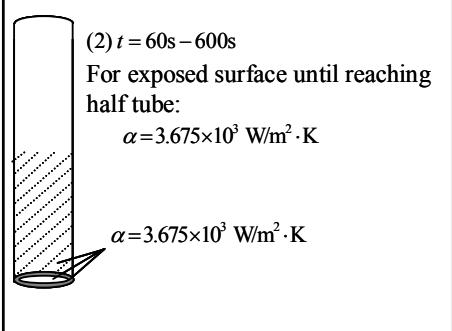


Fig.3 Surface heat transfer as a function of x/a for two-dimensional cylinder in the molten metal with the velocity $u = 25\text{mm/s}$
 (1) Radius $a = 125\text{mm}$ in molten zinc [3]
 (2) Radius $a = 85\text{mm}$ in molten aluminum

When $u = 2\text{mm/s}$, a constant value $\alpha_m = 1.523 \times 10^3 \text{ W/m}^2 \cdot \text{K}$ in Eq. (3) is applied for dipping step by step along the inner and outer surfaces ($r_i = 70\text{mm}$, $r_o = 85\text{mm}$) until reaching half tube. Since it takes 328s for dipping completely, sixteen types of partially dipping models are considered as shown in the Table 3, and the value $\alpha_m = 1.523 \times 10^3 \text{ W/m}^2 \cdot \text{K}$ is applied to the whole surface touching molten aluminum.

Then, the results are shown in Fig.4 (a). The figure indicates the maximum tensile principle stress σ_1 , maximum compressive principle stress σ_3 and maximum stresses components σ_r , σ_θ , σ_z . Since the maximum shear stresses τ_{rz} , $\tau_{\theta z}$, $\tau_{r\theta}$ are within 25% of $\sigma_{z\text{max}}$, only the largest shear stress τ_{rz} is indicated. From Fig. 4 (a) it is seen that $\sigma_{z\text{max}}$ coincides with σ_1 at $t = 20.5\text{s}$, and $\sigma_{z\text{min}}$ coincides with σ_3 at $t = 165\text{s}$. Therefore, only $\sigma_{z\text{max}}$ and $\sigma_{z\text{min}}$ will be discussed later because they are almost equivalent to the maximum stresses σ_1 and σ_3 , respectively. The stress $\sigma_{z\text{max}}$ has the peak value of 128MPa at $t = 20.5\text{s}$. The maximum thermal stress $\sigma_{z\text{max}} = 128\text{MPa}$ does not decrease while half of the tube is dipping into the molten metal. However, the stress decreases gradually after half dipping is finished. Since we use sixteen types of partially

Table 3 Assumption of surface heat transfer coefficient α , $\text{W/m}^2 \cdot \text{K}$

Model	<p>Cylinder model under horizontal dipping (Molten aluminum $T=750^\circ\text{C}$)</p> <p>$r_o = 85\text{mm}$ $r_i = 70\text{mm}$</p> 	<p>Cylinder model under vertical dipping (Molten aluminum $T=750^\circ\text{C}$)</p> <p>$r_o = 85\text{mm}$ $r_i = 70\text{mm}$</p> 
<p>$u = 2\text{mm/s}$</p> <p>For dipping step by step:</p> <p>$\alpha = 1.523 \times 10^3 \text{ W/m}^2 \cdot \text{K}$</p> <p>Step 6</p>  <p>Step 2</p> <p>$\alpha = 1.523 \times 10^3 \text{ W/m}^2 \cdot \text{K}$ given</p>	<p>For dipping step by step until reaching half tube:</p> <p>$\alpha = 1.523 \times 10^3 \text{ W/m}^2 \cdot \text{K}$</p> <p>Step 16</p> <p>$\alpha = 1.523 \times 10^3 \text{ W/m}^2 \cdot \text{K}$ given</p> <p>Step 8</p> <p>Step 2</p> 	
<p>$u = 25\text{mm/s}$</p> <p>(1) $t = 0 - 60\text{s}$</p> <p>Along outer surface $r_o = 85\text{mm}$ $\alpha = (3.675 - 18.13) \times 10^3 \text{ W/m}^2 \cdot \text{K}$ (see Fig. 3)</p> <p>At both ends $z = \pm 650\text{mm}$ $\alpha = 3.675 \times 10^3 \text{ W/m}^2 \cdot \text{K}$</p> <p>Along inner surface $r_i = 70\text{mm}$ $\alpha = 3.675 \times 10^3 \text{ W/m}^2 \cdot \text{K}$</p> <p>$\alpha = 3.675 \times 10^3 \text{ W/m}^2 \cdot \text{K}$</p>  <p>$\alpha = (3.675 - 18.13) \times 10^3 \text{ W/m}^2 \cdot \text{K}$</p> <p>(2) $t = 60\text{s} - 600\text{s}$</p> <p>For all exposed surfaces: $\alpha = 3.675 \times 10^3 \text{ W/m}^2 \cdot \text{K}$ $\alpha = 3.675 \times 10^3 \text{ W/m}^2 \cdot \text{K}$</p> 	<p>(1) $t = 0 - 60\text{s}$</p> <p>Along inner and outer surfaces $r_i = 70\text{mm}$ $r_o = 85\text{mm}$ $z: 0 - 650\text{mm}$ $\alpha = 3.675 \times 10^3 \text{ W/m}^2 \cdot \text{K}$</p> <p>For lower end surface $z = 0\text{mm}$ $\alpha = 18.13 \times 10^3 \text{ W/m}^2 \cdot \text{K}$</p> <p>$\alpha = 3.675 \times 10^3 \text{ W/m}^2 \cdot \text{K}$</p> <p>$\alpha = 18.13 \times 10^3 \text{ W/m}^2 \cdot \text{K}$</p>  <p>(2) $t = 60\text{s} - 600\text{s}$</p> <p>For exposed surface until reaching half tube: $\alpha = 3.675 \times 10^3 \text{ W/m}^2 \cdot \text{K}$</p> <p>$\alpha = 3.675 \times 10^3 \text{ W/m}^2 \cdot \text{K}$</p> 	

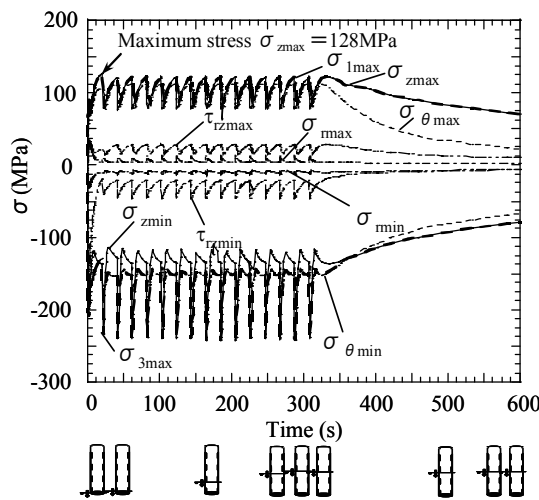


Fig.4 (a) Maximum stresses vs. time relation of vertical tube ($u = 2\text{mm/s}$)

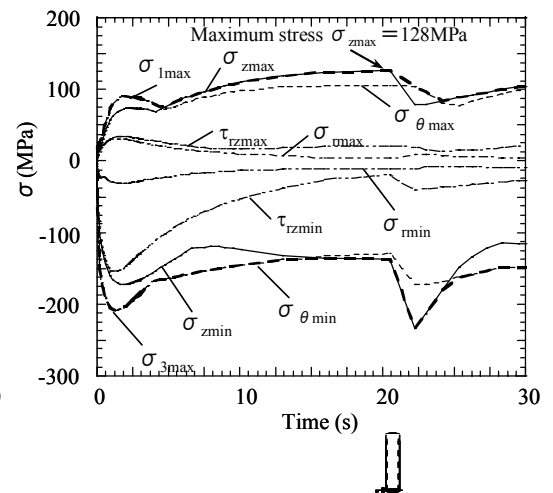


Fig.4 (b) Maximum stresses vs. time relation of vertical tube ($u = 2\text{mm/s}$)

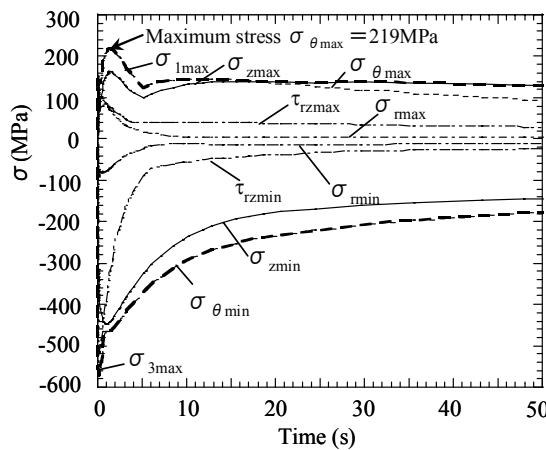


Fig.5 (a) Maximum stresses vs. time relation of vertical tube ($u = 25\text{mm/s}$)

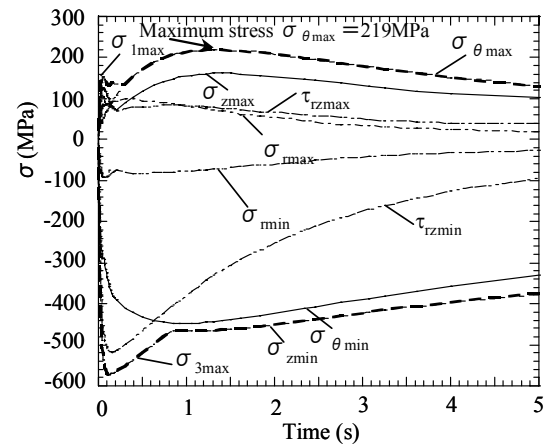


Fig.5 (b) Maximum stresses vs. time relation of vertical tube ($u = 25\text{mm/s}$)

dipping models, fluctuation of stresses appears as shown in Fig. 4 (a).

3.2 Results for Dipping Fast

Thermal stress is considered when the vertical tube in Fig.1 (a) dips into molten aluminum fast at $u = 25\text{mm/s}$. Here, the surface heat transfer is assumed in the following way (see Table 3):

1. When $t = 0 - 60\text{s}$, the minimum value in Fig. 3 $\alpha_m = 3.675 \times 10^3 \text{W/m}^2 \cdot \text{K}$ is applied along the inner and outer surfaces ($r_i = 70\text{mm}$, $r_o = 85\text{mm}$). Also the maximum value in Fig. 3 $\alpha = 18.13 \times 10^3 \text{W/m}^2 \cdot \text{K}$ is assumed at the lower end surface ($z = 0\text{mm}$).
2. When $t > 60\text{s}$, the minimum value in Fig. 3 $\alpha = 3.675 \times 10^3 \text{W/m}^2 \cdot \text{K}$ is assumed for exposed surface until reaching half tube.

Figure 5 (a) shows maximum values of stresses σ_1 , σ_r , σ_θ , σ_z , τ_{rz} . As shown in Fig. 5 (b), the maximum tensile stress $\sigma_1 = \sigma_\theta$ increases in a short time. After taking a peak value $\sigma_{\theta\text{max}} = 219\text{MPa}$ at $t = 1.31\text{s}$, it is decreasing. The maximum value 219MPa is larger than that of 128MPa for dipping slowly.

3.3 Comparison between Dipping Slowly and Fast

The temperature and stress distributions of vertical tubes are indicated in Figs. 6 and 7. Figure 6 shows temperature and stress distributions of σ_z at $t = 20.5\text{s}$, where the

maximum stress $\sigma_{z\max} = 128\text{MPa}$ appears for the tube dipping slowly. Figure 7 shows temperature and stress distributions σ_{θ} at $t = 1.3\text{s}$ where the maximum stress $\sigma_{\theta\max} = 219\text{MPa}$ appears for the tube dipping fast. For dipping slowly at $u = 2\text{mm/s}$, the maximum stress σ_z appears at the inner surface of the tube $r = 70\text{mm}$ just above the dipping level of molten aluminum (see Fig. 6). This is due to the bending moment caused by the thermal expansion of the dipped portion of the tube. On the other hand, for the fast dipping at $u = 25\text{mm/s}$, the maximum stress $\sigma_{\theta\max}$ appears at the inside of the thickness as shown in Fig. 7. This is due to the large temperature difference appearing in the thickness direction. It may be concluded that vertical tubes should be dipped slowly in order to reduce the thermal stresses.

4. Thermal Stress for Horizontal Tube

Thermal stress is considered when the horizontal tube in Fig.1 (b) dips into molten aluminum at the speeds of $u = 2\text{mm/s}$ and $u = 25\text{mm/s}$.

4.1 Results for Dipping Slowly

When $u = 2\text{mm/s}$, a constant value $\alpha_m = 1.523 \times 10^3 \text{ W/m}^2 \cdot \text{K}$ in Eq. (3) is applied for

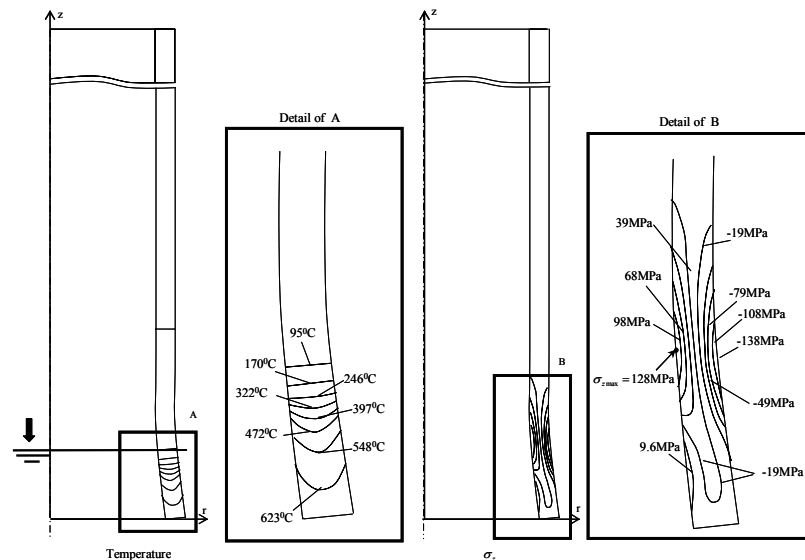


Fig.6 Temperature and stress σ_z distributions of vertical tube ($u = 2\text{mm/s}$ at time $t = 20.5\text{s}$), displacement $\times 50$.

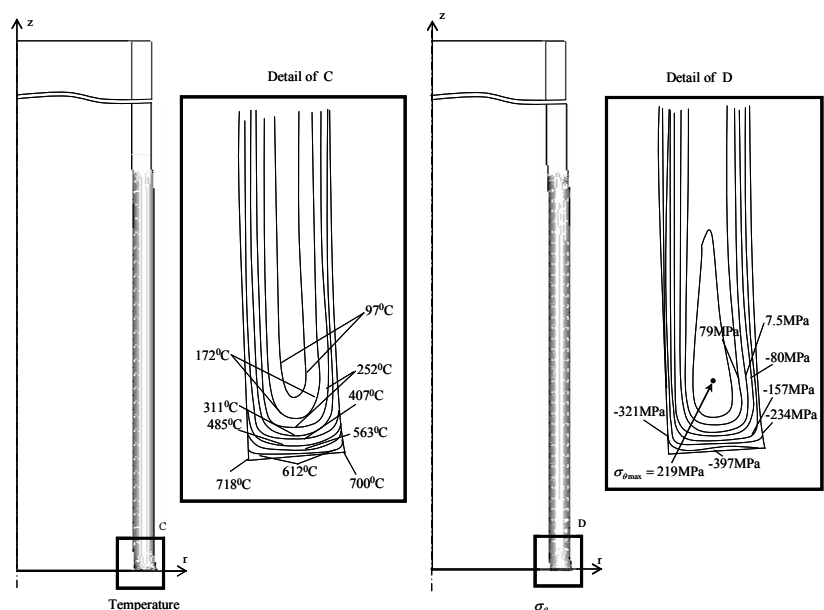


Fig.7 Temperature and stress σ_{θ} distributions of vertical tube ($u = 25\text{mm/s}$ at time $t = 1.3\text{s}$), displacement $\times 50$.

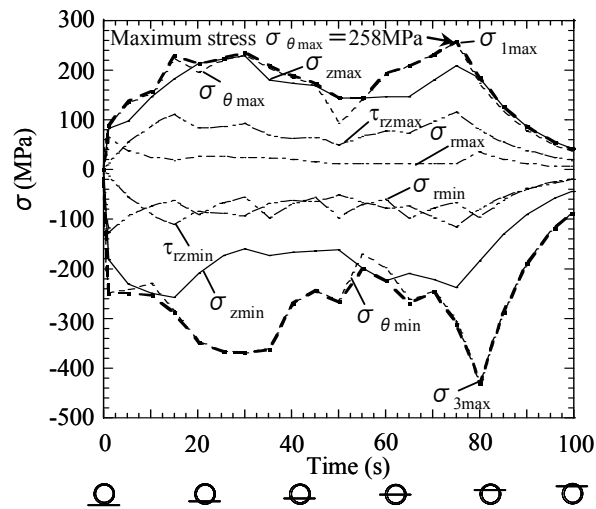


Fig.8 Maximum stresses vs. time relationship of horizontal tube ($u = 2\text{mm/s}$)

dipping step by step along the inner and outer surfaces ($r_i = 70\text{mm}$, $r_o = 85\text{mm}$). Since it takes 210s for dipping completely, six types of partially dipping models are considered as shown in the Table 3, and the value $\alpha_m = 1.523 \times 10^3 \text{ W/m}^2 \cdot \text{K}$ is applied to the surface touching molten aluminum. Figure 8 shows maximum values of stresses σ_1 , σ_r , σ_θ , σ_z , τ_{rz} . In Fig. 8, the maximum tensile stress $\sigma_{\theta\text{max}} = 258\text{MPa}$ appears at $t = 75\text{s}$.

4.2 Results for Dipping Fast

Thermal stress is considered when the horizontal tube in Fig.1 (b) dips into the molten aluminum fast at $u = 25\text{mm/s}$. Here, the surface heat transfer is assumed in the following way:

1. When $t = 0 - 60\text{s}$, the values in Fig. 3 $\alpha = (3.675 - 18.13) \times 10^3 \text{ W/m}^2 \cdot \text{K}$ are applied along the outer surface ($r_o = 85\text{mm}$). Also the minimum value in Fig. 3 $\alpha = 3.675 \times 10^3 \text{ W/m}^2 \cdot \text{K}$ is assumed at the inner surface ($r_i = 70\text{mm}$) and tube ends $z = \pm 650\text{mm}$.
2. When $t > 60\text{s}$, the minimum value in Fig. 3 $\alpha = 3.675 \times 10^3 \text{ W/m}^2 \cdot \text{K}$ is assumed for all exposed surfaces.

Figure 9 (a) shows maximum values of stresses σ_1 , σ_r , σ_θ , σ_z , τ_{rz} . As shown in Fig. 9

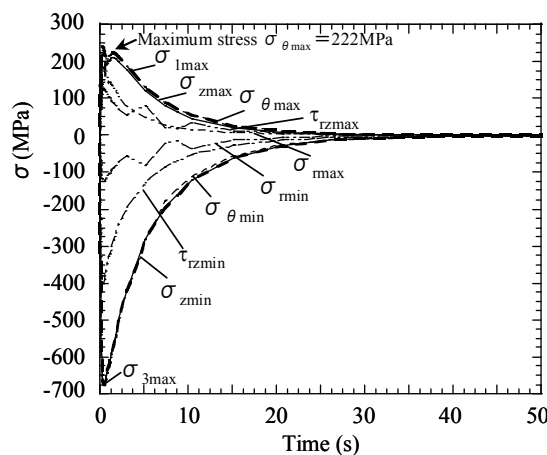


Fig. 9 (a) Maximum stresses vs. time relationship of horizontal tube ($u = 25\text{mm/s}$)

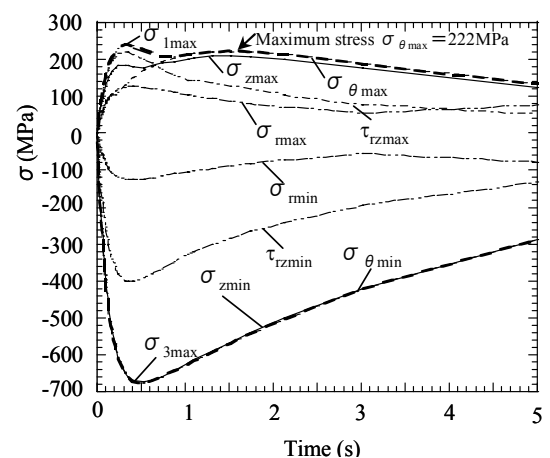


Fig. 9 (b) Maximum stresses vs. time relationship of horizontal tube ($u = 25\text{mm/s}$)

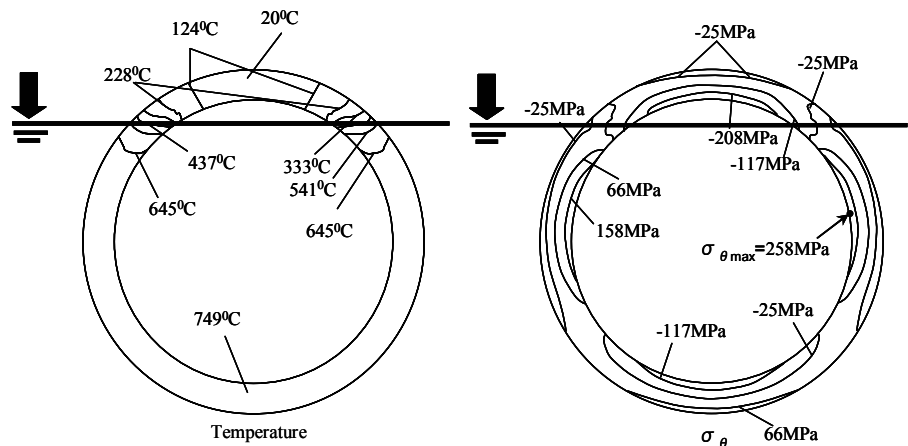


Fig.10 (a) Temperature and stress σ_{θ} distributions of horizontal tube at both ends $z = \pm 650\text{mm}$ ($u = 2\text{mm/s}$ at time $t = 75\text{s}$).

(b) the maximum stress increases in a short time, and has a peak value $\sigma_{\theta\text{max}} = 222\text{MPa}$ at $t = 1.5\text{s}$.

4.3 Comparison between Dipping Slowly and Fast

Figure 10 (a) shows the temperature and stress distributions σ_{θ} for horizontal tube at both ends where $\sigma_{\theta\text{max}} = 258\text{MPa}$ appears at $t = 75\text{s}$ for the tube dipping slowly. Figure 10 (b) shows temperature and stress distributions σ_{θ} near both ends, where $\sigma_{\theta\text{max}} = 222\text{MPa}$ appears at $t = 1.5\text{s}$ for the tube dipping fast.

For dipping slowly, as shown in Fig. 11 (a) the maximum stress $\sigma_{\theta\text{max}}$ appears at the inner surface of the tube ends $z = \pm 650\text{mm}$. In this case the circular cross section becomes elliptical because of temperature difference between the dipped and upper parts. In other words, the maximum stress $\sigma_{\theta\text{max}}$ appears due to asymmetric deformation. For dipping fast as shown in Fig. 11 (b), the temperature and stress distributions are similar to the ones of vertical tube dipping fast in Fig. 7. In other words, for dipping fast, the deformation is almost axi-symmetric. The larger stress appears much more shortly than the case of $u = 2\text{mm/s}$. Therefore, horizontal tubes should dip fast at $u = 25\text{mm/s}$ rather than slowly at $u = 2\text{mm/s}$ to reduce the thermal stress.

5. Comparison between the Results of Vertical and Horizontal Tubes

Table 4 shows the maximum values of tensile stresses for vertical and horizontal tubes. For vertical tube, dipping slowly may reduce the thermal stress because dipping fast causes large temperature difference in the thickness direction of the tube. On the other hand, for horizontal tube, dipping fast may reduce the thermal stress although in this case similar

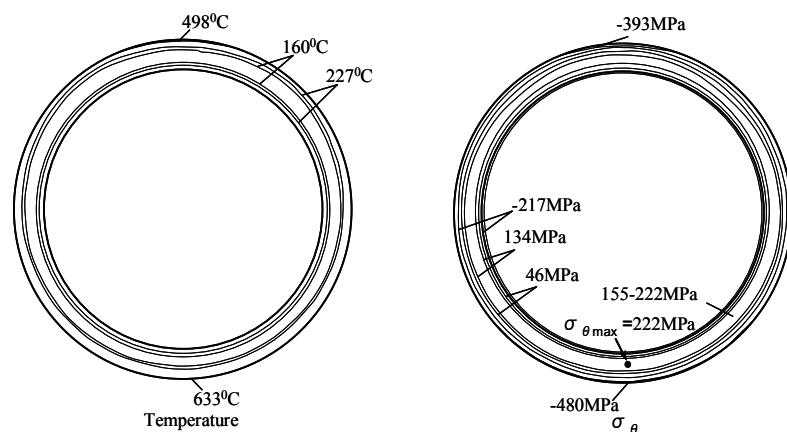


Fig.10 (b) Temperature and stress σ_{θ} distributions of horizontal tube near the both ends at $z = 615\text{mm}$ ($u = 25\text{mm/s}$ at time $t = 1.5\text{s}$).

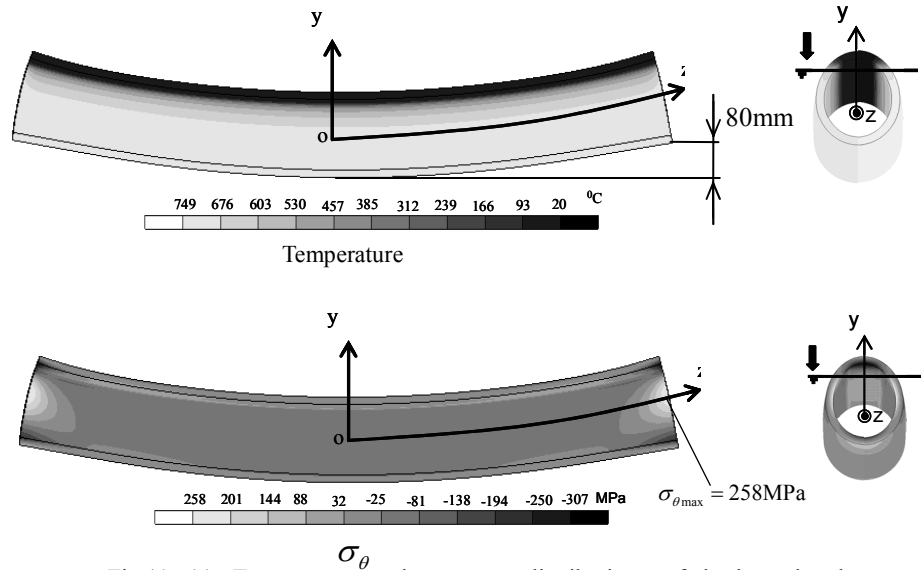


Fig.11 (a) Temperature and stress σ_{θ} distributions of horizontal tube ($u = 2\text{mm/s}$ at time $t = 75\text{s}$), displacement $\times 30$.

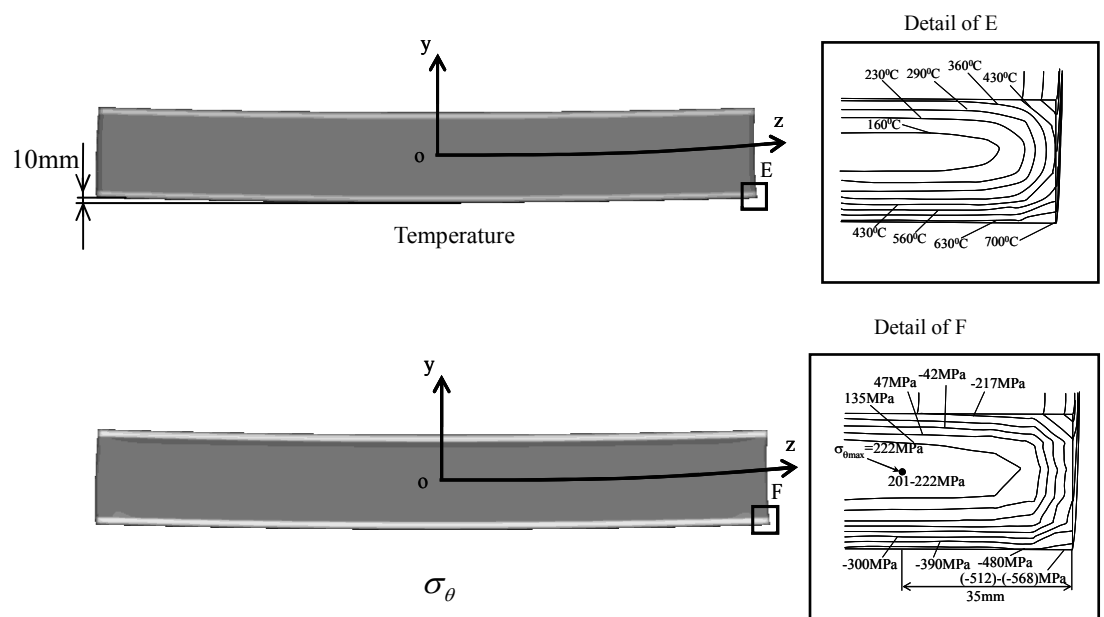


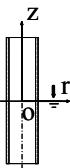

Fig.11 (b) Temperature and stress σ_{θ} distributions of horizontal tube ($u = 25\text{mm/s}$ at time $t = 1.5\text{s}$), displacement $\times 30$.

large temperature difference appears in the thickness direction. Those different conclusions may be explained in terms of deformations of the tube. For vertical tube, the deformation is always axi-symmetric. However, for horizontal tube, dipping slowly causes large asymmetric deformation, which results in the largest $\sigma_{\theta\text{max}}$ at the inner surface of the end of the tube. On the other hand, for fast dipping of horizontal tube, the deformation is almost axi-symmetric.

6. Conclusions

In the recent low pressure die casting machine, the vertical tube called stalk is usually made of ceramics because of its high temperature and corrosion resistances. However, attention should be paid to the thermal stresses when the tube is dipped into the molten aluminum. In this paper, therefore, how to reduce the thermal stress is considered when the tube is installed in the crucible by the application of finite element method. The conclusions

Table 4 Maximum tensile stress of vertical and horizontal tube

	Vertical dipping	Horizontal dipping
Model		
$u=2\text{mm/s}$	$\sigma_{z\text{max}} = 128\text{MPa}$	$\sigma_{\theta\text{max}} = 258\text{MPa}$
$u=25\text{mm/s}$	$\sigma_{\theta\text{max}} = 219\text{MPa}$	$\sigma_{\theta\text{max}} = 222\text{MPa}$

are given as following.

1. For vertical tube, dipping slowly may be suitable for reducing the thermal stresses because dipping fast causes larger temperature difference in the thickness direction, which results in larger thermal stresses.
2. For horizontal tube, however, dipping fast may be suitable for reducing the thermal stress even though it causes larger temperature difference in the thickness direction of the tube.
3. Those different conclusions are explained in terms of deformations of tube. For horizontal tube, dipping slowly causes larger asymmetric deformation, which results in larger $\sigma_{\theta\text{max}}$ at the tube ends.

References

- (1) "The A to Z of Materials" Aluminum Casting Techniques-Sand Casting and Die Casting Processes. (Online), available from <<http://www.azom.com/details.asp?ArticleId=1392>>, (accessed 2008-4-23).
- (2) Bonollo, F., Urban, J., Bonatto, B., and Botter, M., Gravity and Low Pressure Die Casting of Aluminium Alloys: a Technical and Economical Benchmark, *Alluminio E Leghe*, (2005).
- (3) Noda, N.A., Yamada, M., Sano, Y., Sugiyama, S., and Kobayashi, S., Thermal Stress for All-ceramics Rolls used in Molten Metal to Produce Stable High Quality Galvanized Steel Sheet, *Engineering Failure Analysis*, Vol. 15, (2008), pp. 261-274.
- (4) Editorial committee of JSME, *Data of heat transfer*, Tokyo: JSME, (1986), p.323 [in Japanese].
- (5) Nogami, S., Large Sialon Ceramics Product for Structural Use, *Hitachi Metal Report*, Vol.15, (1999), pp.115-120 [in Japanese].
- (6) Korenaga, I., Sialon Ceramics Products used in Molten Aluminum, Sokeizai (1991); 5:12-7 [in Japanese].
- (7) Zukauskas, A., Heat Transfer from Tubes in Cross Flow, In: Hartnett JP, Irvine Jr TF, editors, *Advances in Heat Transfer*, Vol.8, New York: Academic Press, (1972), p. 131.
- (8) Editorial committee of JSME, *Data of heat transfer*, Tokyo: JSME; (1986), p.61 [in Japanese].
- (9) Adachi, T., Tamura, Y., and Yoshioka, T., Techniques of Automatic Operation in Continuous Galvanizing Line, *Kawasaki Steel Technical Report*, Vol.34, (1996), pp. 18-25.
- (10) Nishimura, K., Katayama, K., Kimura, T., Yamaguchi, T., and Ito, M., Newly Develop Techniques for Improving the Quality of Continuous Hot dip Plating Strips, *Hitachi Technical Report*, Vol. 65(2), (1983), pp. 121-126 [in Japanese].